

Article

Fibre Individualisation and Mechanical Properties of a Flax-PLA Non-Woven Composite Following Physical Pre-Treatments

Maxime Gautreau ¹, Antoine Kervoelen ², Guillaume Barteau ², François Delattre ³, Thibaut Colinart ² ,
Floran Pierre ⁴, Maxime Hauguel ⁴, Nicolas Le Moigne ⁵ , Fabienne Guillon ¹, Alain Bourmaud ² 
and Johnny Beaugrand ^{1,*} 

- ¹ Biopolymères Interactions Assemblages (BIA), INRA, Rue de la Géraudière, F-44316 Nantes, France; maxime.gautreau@inrae.fr (M.G.); fabienne.guillon@inrae.fr (F.G.)
 - ² Research Institute Dupuy De Lôme (IRDL), University Bretagne Sud, UMR CNRS 6027, F-56100 Lorient, France; antoine.kervoelen@univ-ubs.fr (A.K.); guillaume.barteau@univ-ubs.fr (G.B.); thibaut.colinart@univ-ubs.fr (T.C.); alain.bourmaud@univ-ubs.fr (A.B.)
 - ³ Unité de Chimie Environnementale et Interactions sur le Vivant, Littoral Côte d'Opale University, UR 4492, UCEIV, SFR Condorcet FR CNRS 3417, 145 Avenue Maurice Schumann, 59140 Dunkerque, France; francois.delattre@univ-littoral.fr
 - ⁴ Eco-Technilin SAS, ZA Caux Multipôles, 76190 Valliquerville, France; floran@eco-technilin.com (F.P.); maxime@eco-technilin.com (M.H.)
 - ⁵ Polymers Composites and Hybrids (PCH), IMT Mines Ales, 30100 Alès, France; nicolas.le-moigne@mines-ales.fr
- * Correspondence: johnny.beaugrand@inrae.fr



Citation: Gautreau, M.; Kervoelen, A.; Barteau, G.; Delattre, F.; Colinart, T.; Pierre, F.; Hauguel, M.; Le Moigne, N.; Guillon, F.; Bourmaud, A.; et al. Fibre Individualisation and Mechanical Properties of a Flax-PLA Non-Woven Composite Following Physical Pre-Treatments. *Coatings* **2021**, *11*, 846. <https://doi.org/10.3390/coatings11070846>

Received: 23 June 2021

Accepted: 11 July 2021

Published: 14 July 2021

Publisher's Note: MDPI stays neutral with regard to jurisdictional claims in published maps and institutional affiliations.



Copyright: © 2021 by the authors. Licensee MDPI, Basel, Switzerland. This article is an open access article distributed under the terms and conditions of the Creative Commons Attribution (CC BY) license (<https://creativecommons.org/licenses/by/4.0/>).

Abstract: Pre-treatments for plant fibres are very popular for increasing the fineness of bundles, promoting individualisation of fibres, modifying the fibre-matrix interface or reducing water uptake. Most pre-treatments are based on the use of chemicals and raise concerns about possible harmful effects on the environment. In this study, we used physical pre-treatments without the addition of chemical products. Flax tows were subjected to ultrasound and gamma irradiation to increase the number of elementary fibres. For gamma pre-treatments, a 20% increase in the number of elementary fibres was quantified. The biochemical composition of pre-treated flax tows exhibited a partial elimination of sugars related to pectin and hemicelluloses depending on the pre-treatment. The hygroscopic behaviour showed a comparable decreasing trend for water sorption-desorption hysteresis for both types of pre-treatment. Then, non-woven composites were produced from the pre-treated tows using poly-(lactid) (PLA) as a bio-based matrix. A moderate difference between the composite mechanical properties was generally demonstrated, with a significant increase in the stress at break observed for the case of ultrasound pre-treatment. Finally, an environmental analysis was carried out and discussed to quantitatively compare the different environmental impacts of the pre-treatments for composite applications; the environmental benefit of using gamma irradiation compared to ultrasound pre-treatment was demonstrated.

Keywords: flax tows; ultrasound; gamma treatment; DVS; environmental analysis; mechanical properties; composite materials

1. Introduction

The intensification of global warming coupled with a gradual depletion of petro-sourced resources is pushing our societies and industries to use an increasing number of biomass resources in an ecologically responsible approach. The composite materials sector is not an exception to this trend; for several decades, plant fibres, especially flax, have offered a solution to replace predominant synthetic reinforcements, such as glass fibres. Indeed, flax fibres have some advantages: a lower density [1], specific mechanical properties equivalent to glass fibres [2,3] and a natural and renewable origin. Generally, the

use of flax fibres makes it possible to reduce the carbon footprint of performance composite materials [4], thus enables one to obtain a less impactful life cycle.

Flax processing provides a range of products of different qualities. At the scutching step, good-quality scutched fibres are produced but also low-cost and qualitative scutching tows, which comprise a mixture of elementary fibres, fibre bundles and shives [5]. In industry, they are mainly used for the production of non-woven preforms. These products, manufactured at low cost [6] and in high volume, are particularly popular in the automotive sector to design and produce non-structural interior composite parts [7]. Currently, such preforms are made using a mix of plant fibres and thermoplastic fibres, such as poly-(propylene) (PP), which has good mechanical properties as well as a low melting temperature, which is an important parameter to prevent plant fibre damage during the processing stage [8,9]. To improve the end of life of these materials [10], it is interesting to study the coupling of flax fibres with a biobased and biodegradable polymer matrix such as poly-(lactid) (PLA) or poly-(β -hydroxybutyrate) (PHB).

Cellulose is the main component of flax fibres, which varies in content between 50% and 80% depending on the variety considered [11]. Other non-cellulosic components are hemicelluloses (between 11% and 20%), pectins (2% and 8%) and lignins (approximately 1%–3%). The structure of an elementary flax fibre is characterised by a primary wall, a secondary wall divided into several sub-layers, generally 3, denoted S1, S2 and S3, and a cavity in its centre called the lumen [12]. The thickest S2 sub-layer (5–10 μ m) largely influences the mechanical properties of the fibre. The cohesion of elementary fibres within fibre bundles is ensured by the pectin-rich middle lamella [13]. However, hemicelluloses and lignins can also be found in this latter part. Non-wovens are made using tows, which contain both elementary fibres and bundles but also some woody sticks to a certain extent; these materials are named shives and are considered contaminants by materials engineers. The shives composition and mechanical properties strongly differ from those of technical fibres [14,15], and contain a reduced fraction of cellulose and more lignin.

For industrial materials, mechanical properties are among the predominant characteristics determining future functionalities and uses. Non-woven composites have interesting mechanical properties; according to Ashby material charts, they are superior to injection-moulded composites thanks to longer fibres but inferior to unidirectional composites (UDs) [16]. In general, in plant fibre-reinforced composites, individualisation of fibre bundles into elementary fibres is one of the key parameters to obtain good mechanical properties. Indeed, the middle lamella, which ensures fibre cohesion within fibre bundles, is an area of weakness due to its poor mechanical properties [17]. In addition, an aspect ratio (length/diameter) for the fibres of greater than 10 is considered the minimum value for efficient stress transfer during mechanical stress loading [18]. As an example, a positive impact of individualisation was observed on the mechanical properties of flax/epoxy UD composites [19]. These different elements show that by damaging or solubilising the middle lamella, an increase in elementary fibre content, and, at the same time, a decrease in fibre bundle content are promoted. At the composite scale, this modification of the architecture of the fibres allows for a larger specific fibre/matrix interfacial area as well as an optimised aspect ratio, and; therefore, better mechanical properties.

To induce this individualisation for fibre bundles, several types of pre-treatments exist, potentially used as alternatives or post-assisting to retting [20]. First, chemical pre-treatments, such as the use of chelating agents such as ethylenediaminetetraacetic acid (EDTA), are frequently used for the defibrization of plant fibres. Chelation removes calcium ions from the pectins of the middle lamella [21]. Alkaline treatments of the NaOH or KOH type are commonly used to eliminate non-cellulosic components of the fibre, such as hemicelluloses and pectins [22]. However, using chemical agents used to modify plant fibres penalise their eco-friendly aspect and can possibly reduce fibre and composite performance [23]. In this regard, physical and chemical-free pre-treatments are needed to increase the individualisation for fibre bundles. Ultrasonic treatment of hemp fibres has been shown to reduce the diameter of fibre bundles by removing pectic and

hemicellulosic structures [24]. This elimination of cell-wall polymers is possibly due to the phenomenon of cavitation; the asymmetric implosion of bubbles near the material results in turbulence, which can damage certain binding constituents, such as those in the middle lamella in particular. Ultrasound treatment allows further changes to the fibre. In fact, ultrasonically treated fibres show a significant reduction in water sorption [25] as well as a delignification process [26]. Other physical pre-treatments that do not involve immersion in a solvent such as gamma irradiation can be used to promote individualisation for fibre bundles. The use of gamma irradiation for lignocellulosic fibres shows interesting effects. Scanning Electron Microscope (SEM) observations showed that the primary wall and the middle lamella of henequen fibres are strongly impacted by gamma irradiation [27]. In addition, non-cellulosic polymers such as low DP hemicelluloses, impurities and waxes undergo degradation at low irradiation doses (<10 kGy) [28]. Therefore, it appears to be possible to preferentially degrade the pectins in the middle lamella while preserving the cellulose structure and thermal and mechanical properties of plant fibres, providing that low irradiation doses are used (<30 kGy) [28]. Gamma irradiation can decrease water uptake for fibres treated at low doses thanks to the removal of hydrophilic components; jute fibres irradiated and then immersed in water for 30 days indicate a 14% drop in water absorption [29]. Gamma irradiation can also promote fibre/matrix interfacial adhesion by modifying the surface topography of plant fibres and enhancing their roughness [27], thus allowing better mechanical interlocking and a potential increase in interphase properties with a polymer matrix.

The aim of this work is to apply free-of-chemicals pre-treatments to maximise the environmental benefit of flax technical fibres. Two physical pre-treatments: ultrasound and gamma irradiation were applied to flax tows with the aim of increasing the specific surface area and aspect ratio of the flax reinforcements. The efficiency of these physical pre-treatments was evaluated by monitoring the individualisation into elementary fibres and the reduction in the size of the fibre bundles by means of a dynamic morphological analysis. In addition, the chemical composition and water uptake of (un)treated tows was evaluated. Then, treated flax tows were used to produce non-woven flax-PLA composites, and the impact of pre-treatments on their microstructure and mechanical properties was studied. Finally, an environmental analysis of the various treatments was undertaken to assess whether or not the environmental impact of the pre-treatments is justified by the potential gain in the mechanical properties of the related composites.

2. Materials and Methods

2.1. Materials

2.1.1. Flax Tows

Flax tows (*Linum usitatissimum* L.) from the Bolchoi variety were supplied by Depestele (Bourguebus, France). Flax plants were cultivated in 2017 (Normandy, France) and dew-retted in the field. These plants had a length of approximately 80 mm and a shive rate less than 5%. This sample was named Native, no-treated flax tows.

2.1.2. Flax-PLA Non-Woven Preforms

The non-woven preforms were composed of 50:50 wt% of flax tows and PLA fibres and manufactured in October 2020 by the EcoTechnilin Company (Yvetot, France). PLA fibres had a length of 60 mm and a diameter of approximately 30 μm . Three non-woven preforms were produced with the different batches of flax: untreated, gamma irradiation and ultrasound pre-treated. All non-woven preforms had a basis weight of approximately 100 g/m².

2.1.3. Composite Manufacturing

The flax-PLA non-woven composites were produced by hot pressing using a Darragon 35T hydraulic press. The dimensions of the composite plates were 160 \times 160 \times 1.5 mm³. The time-temperature-pressure cycle used is described as follows: Heat up to 190 °C, 3 min

of preheating on contact, followed by the application of 50 bar pressure for 3 min at 190 °C, and, finally, a 15 min cooling under pressure to reach 10 °C.

2.2. Physical Pre-Treatments

2.2.1. Ultrasound

Ultrasound pre-treatment were carried out using a semi-pilot tank (SinapTec, Lezennes, France) at the Université du Littoral (Dunkerque, France). The pre-treatment parameters are an output power of 2500 W and a frequency of 20 kHz. The semi-pilot tank can contain a volume of 50 L of water. Ultrasonic pre-treatment requires immersion in a solvent for the propagation of ultrasonic waves. The pre-treatment was carried out by immersion in water during 30 min. This duration of the pre-treatment was established by preliminary tests, which showed the best individualisation for this duration (data not shown). For ultrasound pre-treatment, 2.5 kg of tows was used. The ultrasound pre-treated tows were named US 30 min. A chiller with an air-cooled refrigerating unit and circulation pump (Unichiller 025 OLE, Huber, Offenburg, Germany) was used to maintain the water temperature at approximately 25 °C during the pre-treatment. After the pre-treatment, the flax tows were dried overnight in an oven (BD 56, Binder GmbH, Tuttlingen, Germany) at 60 °C.

2.2.2. Gamma Irradiation

Gamma irradiation was carried out industrially by the company Ionisos (Dagneux, France). To preserve the fibre structure and physical properties [28], a low dose of 5–7 kGy was applied to approximately 2.5 kg of flax tows; this sample was named Gamma. Gray is the unit derived from the international system of units for absorbed dose. A Gray represents the energy of ionising radiation from one joule to a homogeneous medium with a mass of one kilogram.

2.3. Characterisation

2.3.1. Particle Size Analysis

The morphology of the particles was studied with an automated dynamic morphological analyser (SympaTec GmbH, Clausthal, Germany) called QICPIC and further use in the text as its model name by measuring the particle diameter (DIFI). DIFI was defined as the quotient of the total projection area and the sum of all the lengths of the branches of the fibre backbone:

$$\text{Diameter} = \frac{\text{total projection area}}{\text{sum of the lengths of all the tendrils}} \quad (1)$$

Flax tows were studied in a water solution using a dispersion unit, LIXELL (SympaTec GmbH, Clausthal, Germany), to prevent particle aggregation. Each sample was weighed to approximately 50 mg and then pre-dispersed in 5 mL of ethanol and then 45 mL of distilled water before undergoing further dispersion using an ultrasound probe (Vibra-Cell™ 75022, Bioblock Scientific, Hampton, NH, USA). The solution was finally dispersed in 950 mL of distilled water under magnetic stirring. All samples were analysed using a M7 lens, which allows precise measurement of particles with dimensions ranging from 4.2 to 8665 µm (ISO). The number of particles analysed varied between hundreds of thousands to a million depending on the samples. For each sample, measurements were carried out in triplicate to ensure the reproducibility of the data. PAQXOS software (SympaTec GmbH, Clausthal, Germany) was used to calculate the particle diameter (DIFI).

2.3.2. SEM Observations

SEM images of fibres and composites were recorded by using a Jeol JSM IT-500 HR (JEOL Ltd., Tokyo, Japan). All samples were spin coated with gold for 180 s using an Edwards Scancoat Six device before observations. Secondary emission electrons were used, with an accelerating voltage of 3.0 kV.

For the composite cross-section observations, a section of composite was inserted into a mixture of 34 g of catalyser and 100 g of epoxy resin. The sample was placed overnight in an oven at 50 °C to promote crosslinking. Then, the surface of the sample, which was subsequently characterised using a SEM was polished using an automatic polisher (TegraForce-5, Struers, Copenhagen, Denmark). Several polishes were carried out with different polishing times and grains: 60 s/500, 90 s/800, 120 s/1000, 150/1200, 180 s/2000 and 210 s/4000.

2.3.3. Monosaccharide Composition

The quantification and identification of the neutral monosaccharides constituting flax tows was carried out by gas chromatography after acid hydrolysis and conversion of the monomers into alditol acetates [30]. A DB 225 capillary column (J&W Scientific, Folsom, CA, USA; temperature 205 °C, carrier gas H₂) was used to perform the chromatography. For calibration, a range of glucose solutions and inositol as an internal standard were used. Approximately 12 g of fibres in total were tested, and the measurements were performed in duplicate.

2.3.4. Water Sorption/Desorption

The sorption and desorption isotherms for water were established with a dynamic vapour sorption device (IGAsorpt-HT, Hidden Isochema, Warrington, UK). The flax tows were cut to approximately 3–4 mm, and 25 mg was placed in a microbalance located in the hermetic reactor. Prior to adsorption, the samples were dried at 105 °C for 1 h. Inside the reactor, the temperature and relative humidity (RH) were controlled. The sorption/desorption sequence was programmed as follows: Increase from 0% to 90% RH, and then decrease to 0% RH at 20% RH steps. For each RH step, the sample mass was continuously measured until equilibrium was reached (i.e., when the mass variation became less than 0.1 µg/min over a 1 h window).

2.3.5. Mechanical Properties of the Composite Plates

The specimens were cut from the manufactured composite plates with a milling machine. For each plate, five tensile (20 × 8 mm²), four bending (80 × 10 mm²) and two SEM (20 × 20 mm²) test specimens were cut. The tensile properties of the flax-PLA non-woven composites were determined in accordance with the ISO 527 standard. The uniaxial tensile tests are performed in the static state during loading. An MTS Criterion Model 42 machine (MTS, Eden Prairie, MN, USA) with an MTS extensometer (nominal length 25 mm) was used with a 5 kN load cell (MTS, Eden Prairie, MN, USA) and a constant displacement rate of 1 mm/min. Load cell indicated the maximum force that the (traction) cell can provide. Five specimens were tested for each composite.

The bending properties of flax-PLA non-woven composites were determined according to the ISO 178 standard using an MTS Synergie 1000 R/T apparatus (MTS, Eden Prairie, MN, USA). The three-point bending tests were carried out at a constant displacement rate of 1 mm/min with a 250 N load cell. Four specimens were tested for each composite.

2.4. Environmental Analysis

The purpose of this study was to determine the environmental impacts of two physical treatments applied to flax tows: ultrasound (see Section 2.2.1) and gamma irradiation (see Section 2.2.2). Here, a simplified environmental analysis was conducted and not a full LCA (ISO 14044). The model was realised with the software Simapro. The Ecoinvent V_{3.5} database was used. The system boundaries are based on the cradle-to-gate approach and are represented in Figures 1 and 2. The locations of the production sites were included. The flax tows data were obtained from the company Depestele, located in Normandy, France as part of the program FARBioTY. The model works by mass allocation, which means that if a process has several products, the impact of each of the products is allocated in proportion to its mass. The studied impacts are abiotic depletion, global warming,

ozone layer depletion, human toxicity, acidification and eutrophication based on the CML 2 baseline 2000 calculation method. The energy consumption, fossil and nuclear, was calculated with the Cumulative Energy Demand V1.11 method. Evaluations of indicators are available in the literature [31]. The results are presented as diagrams with a relative scale. Due to the uncertainties, for the same environmental indicator, if the difference between two studied pre-treatments is less than 5%, they are considered equal. Interventionary studies involving animals or humans, and other studies that require ethical approval, must list the authority that provided approval and the corresponding ethical approval code.

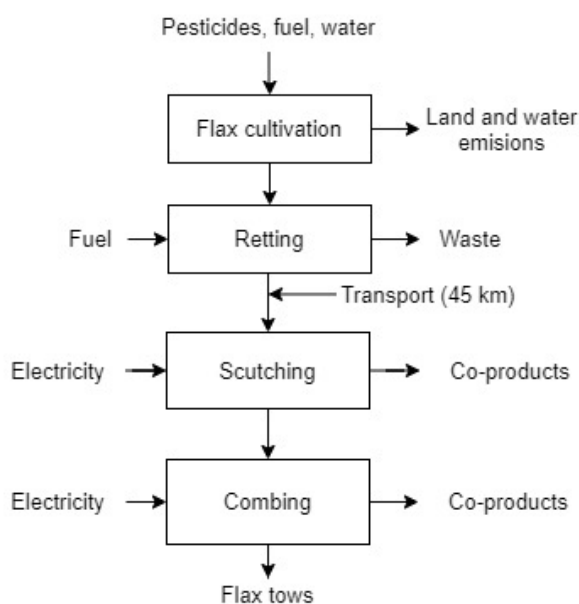


Figure 1. Flow chart of flax tows production.

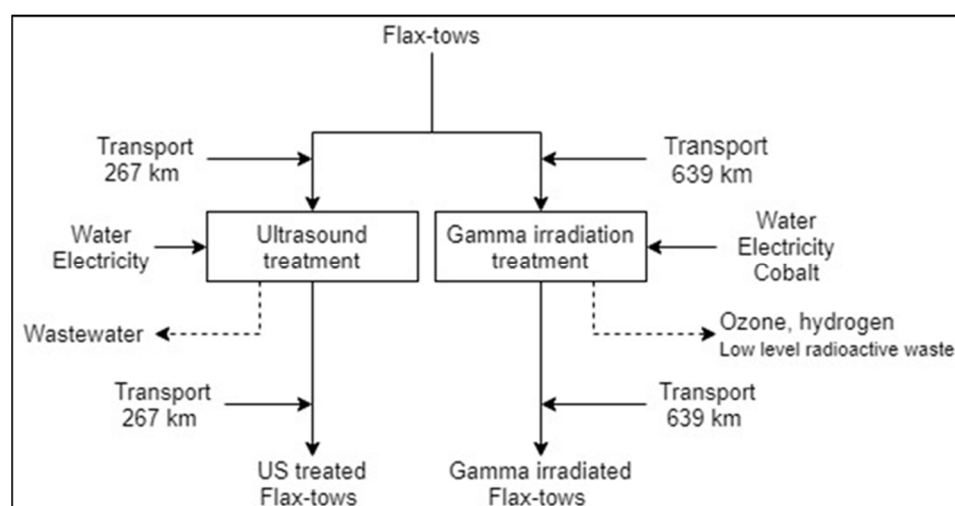


Figure 2. Flow chart for ultrasound and gamma irradiation pre-treatments.

3. Results

3.1. Individualisation of Pre-Treated Flax Tows

The distribution of the fibre element diameters for the Native, Gamma and US 30 min samples is illustrated in Figure 3. Figure 3b clearly shows the presence of larger fibre bundles for the US 30 min treated sample with a last decile of $159.9 \pm 5.8 \mu\text{m}$ compared to $140.6 \pm 15.9 \mu\text{m}$ for the Native sample. The lowest median diameter of $54.4.9 \pm 3.0 \mu\text{m}$

was obtained for the gamma-treated sample, compared to a value of $66.8 \pm 11.2 \mu\text{m}$ for the Native sample. To visualise the evolution of the smallest diameters for which very few differences are visible on box plots, another representation for the evolution of flax tow diameters is given in Figure 4.

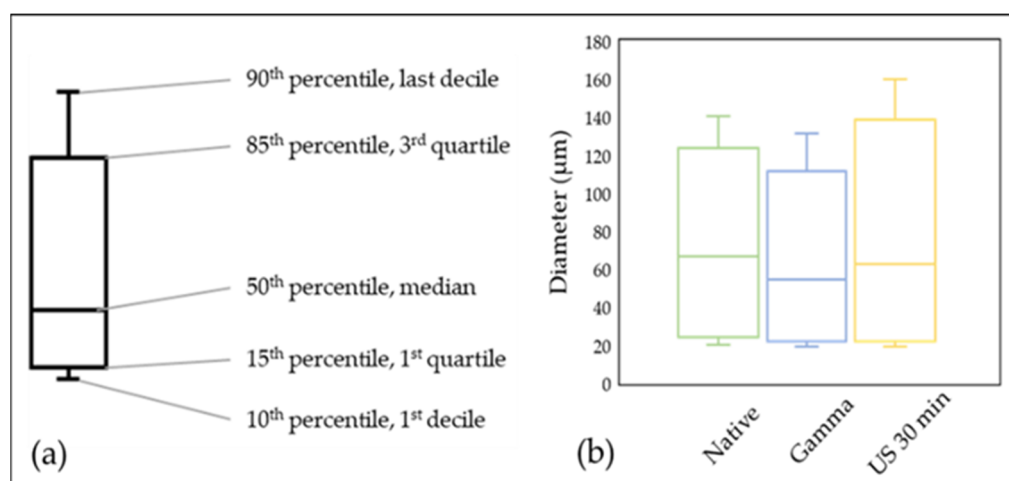


Figure 3. (a) Signification of a box-plot representation; (b) diameter distribution of native and pre-treated flax tows.

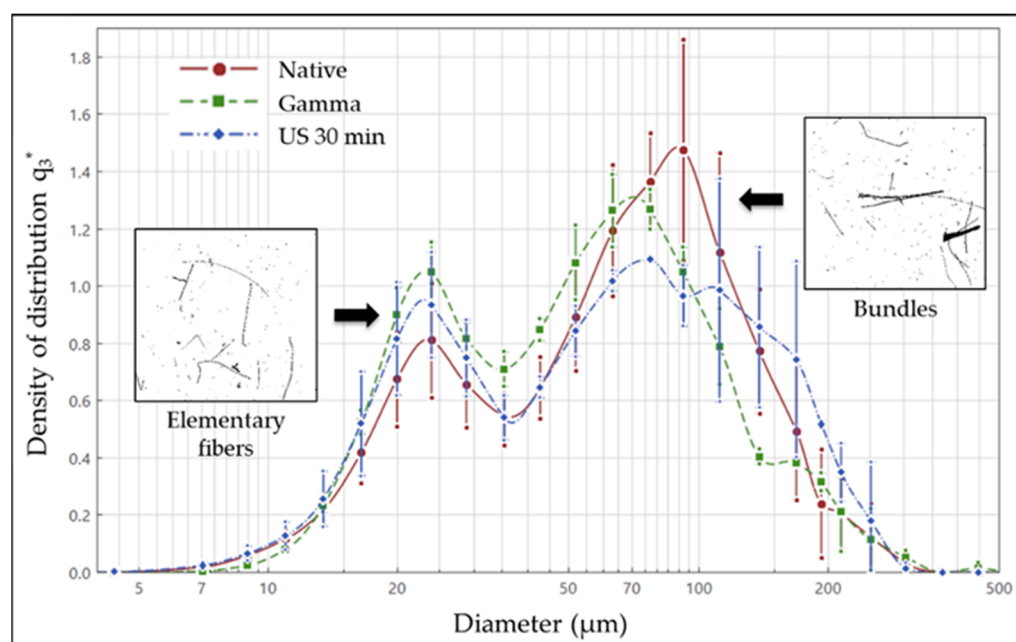


Figure 4. Diameter density of native and pre-treated flax tows and binary images of elementary fibres and fibre bundles in the two insets.

Figure 4 shows the distribution of the fibre element diameters for native and pre-treated tows treated with gamma irradiation and ultrasound, respectively. First, all the plots show a bimodal distribution of diameters with a first peak centred at approximately 25 μm and a second peak located towards diameters of 70–100 μm , corresponding to elementary fibre and fibre bundles, respectively. Representative picture illustrations obtained by the morphometric analyser (QICPIC) are encrusted in Figure 4. The red curve related to native tows (Native) has the highest peak attributed to fibre bundles with a density close to 1.5 for diameters of 90 μm . For the gamma pre-treatment (Gamma), the peak related

to the fibre bundles shows a distribution density of 1.3 for a diameter of 70 μm . The density was 1.1 for a diameter of 75 μm for tows pre-treated by ultrasound (US 30 min). Therefore, a reduction in the diameters of the fibre bundles for the Gamma and US 30 min samples was observed. However, Figure 4 indicates a greater distribution density for the US 30 min sample than the Native sample for fibre bundles exceeding 150 μm in diameter, suggesting an agglomeration of fibres during or after ultrasound pre-treatment. Then, the peak at approximately 25 μm shows an opposite tendency to that for a greater diameter at 70–100 μm . In fact, this peak related to the elementary fibres indicates higher distribution densities for the pre-treated tows, with values of 1.05, 0.95 and 0.8 for the Gamma, US 30 min and Native samples, respectively; hence, highlighting the positive impact of both treatments on fibre individualisation. The gamma pre-treatment clearly results in a decrease in the median diameter (Figure 3b) due to the increase in the number of elementary fibres and the decrease in the number of fibre bundles. For the US 30 min sample, the median diameter is similar to that of the Native sample because the higher number of elementary fibres is counterbalanced by the appearance of fibre bundles with a diameter of more than 150 μm . Thus, gamma irradiation pre-treatment allows for a significant increase in the number of elementary fibres of approximately 20%. This increased number of elementary fibres is slightly less pronounced for ultrasound pre-treatment at +15%.

Figure 5 shows typical SEM images of the three flax tow samples. All images show fibre bundles, but the fibre individualisation differs depending on the sample considered. Indeed, the middle lamella for the Gamma and US 30 min samples is much less visible on the surface of the fibres (Figure 5b,c) than for the Native sample (Figure 5a). Pre-treatments appear to be effective in partially removing the middle lamella and promoting fibre individualisation; these qualitative observations support the diameter measurements obtained with the automated morphometric analyser. However, fibre individualisation was not fully achieved, even after the pre-treatments. Indeed, the middle lamella appears to be still present in the core of the fibre bundles. The distribution density for the fibre bundles (i.e., diameter of 70–100 μm) remains quite high. We can, nevertheless, suppose that, even if present, the middle lamella are weakened by the pre-treatments and might be more easily broken during composite manufacturing, especially if shearing is applied upon processing.

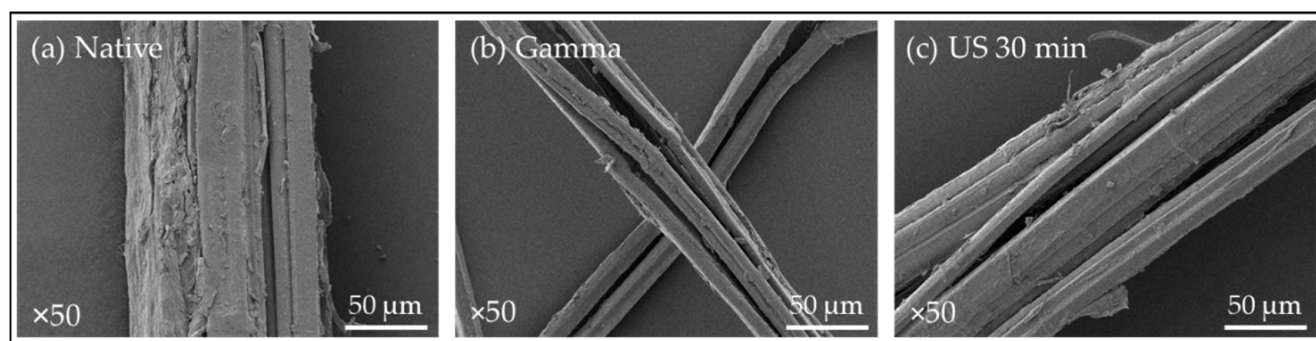


Figure 5. SEM observations ($\times 50$) of tows (a) Native; (b) Gamma; (c) US 30 min.

3.2. Monosaccharide Composition of Flax Tow Samples

The impact of the two pre-treatments on the monosaccharide composition was investigated. Figure 6 shows the percentages of each monosaccharide for the three samples, except glucose for the sake of readability (see Table 1 for glucose).

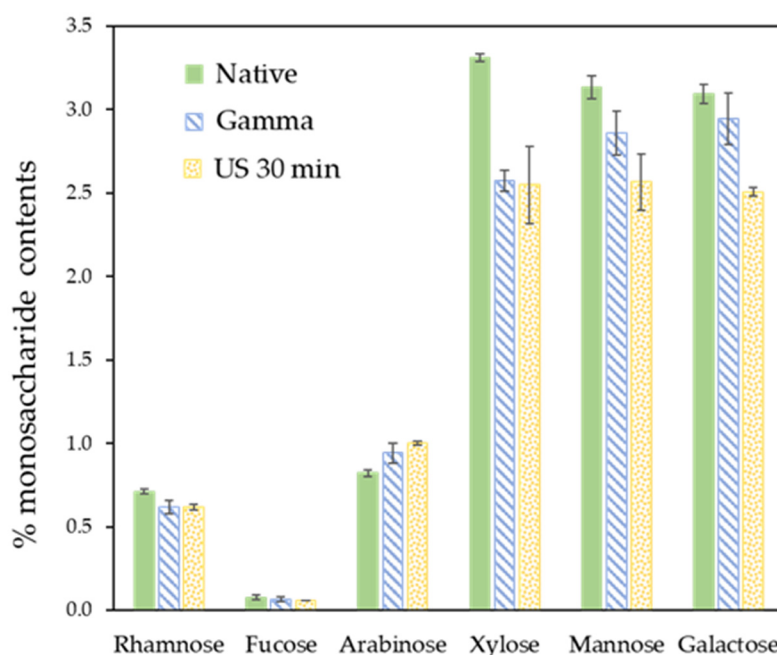


Figure 6. Monosaccharide contents for native and pre-treated flax tows.

Table 1. Glucose contents of Native, Gamma and ultrasound pre-treated flax tows.

Samples	Glucose (%)
Native	68.1 ± 0.9
Gamma	65.5 ± 1.2
US 30 min	64.4 ± 2.1

For rhamnose (Rha) and fucose (Fuc), few differences appeared between pre-treated and native tows. The Rha value ranges between 0.6% and 0.7% for the Gamma and Native samples, respectively. The value of Fuc is very low at approximately 0.065% for the three samples. Both Rha and Fuc monosaccharides are generally associated with pectic structures. The other four sugars quantified—arabinose (Ara), xylose (Xyl), mannose (Man) and galactose (Gal)—show more differences between the three samples. For Xyl, Man and Gal, the same trend is observed with a decrease in the percentage of monosaccharides for both pre-treatments. The most significant decrease occurs for Xyl, which shows a decrease from 3.3% to 2.5% for the Native and US 30 min samples, respectively (i.e., a 25% decrease). For Man, the values obtained for the Native, Gamma and US 30 min samples are 3.1%, 2.8% and 2.6%, respectively. Regarding Gal, the US 30 min sample has the smallest content, followed by the Gamma and Native samples at 2.5%, 2.8% and 3.1%, respectively. Of these three sugars associated with hemicellulosic structures, ultrasound pre-treatment shows the best impact with the lowest monosaccharide values. Finally, the opposite trend is observed for Ara; the highest Ara content is obtained for the US 30 min sample with a value of 1% versus 0.8% for the Native sample. This slight increase in Ara content actually corresponds to compensation for the loss of other monosaccharides.

The percentage of glucose in the three samples is shown in Table 1. The Native sample has the highest glucose level at 68.1%. The two pre-treated samples, Gamma and US 30 min, contain relatively similar glucose levels of 65.5% and 64.4%, respectively. The two pre-treatments do not appear to have too much impact on the glucose, which is generally associated with cellulose. However, this loss of glucose can also be associated with a decrease in hemicelluloses. In both cases, the structural integrity of the flax tow appears to have been preserved. Therefore, the pre-treatments do not damage the structural polysaccharides too much.

3.3. Hygroscopic Behaviour of Pre-Treated Flax Tows

Figure 7 shows the sorption-desorption behaviour of water vapour for the different samples. Differences are visible in Figure 7a,b comparing the pre-treated tow with the native tow. The Native sample has a greater sorption capacity than the Gamma and US 30 min samples. Indeed, for a relative humidity (RH) equal to 90%, the mass difference for the Native, Gamma and US 30 min samples is 17.8%, 15.3% and 15.7%, respectively. In addition, the sorption-desorption behaviour of the gamma and US 30 min pre-treated samples appears to be very similar, as shown in Figure 7c.

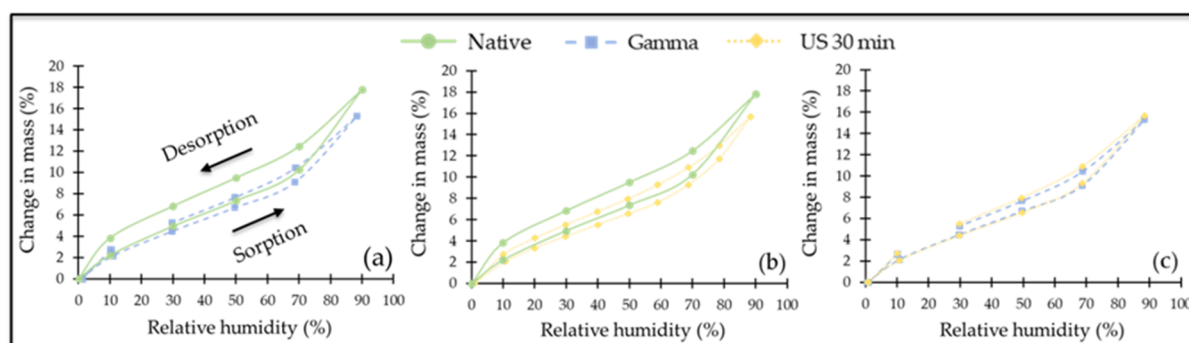


Figure 7. Comparison of sorption-desorption curves for (a) Native and Gamma samples; (b) Native and US 30 min samples; (c) Gamma and US 30 min samples.

Natural fibres belong to the type IV material classification of the International Union of Pure and Applied Chemistry (IUPAC). It is known that the sorption and desorption curves are not superimposable for the same sample [32]. The gap between these two curves (i.e., the hysteresis area) is calculated by subtracting the desorption curve area from the sorption curve area. The hysteresis area data are shown in Table 2. The hysteresis area for the native sample is 149 versus roughly half this value (73) for the Gamma sample and a much lower value (96) for the US 30 min sample. A decreased hysteresis area indicates significant structural changes. The gamma irradiation pre-treatment appears to have the most noticeable effect on decreasing the water uptake and hysteresis between the sorption-desorption curves. The elimination of pectic and hemicellulosic compounds due to the two pre-treatments is responsible for the hygroscopic behaviour of flax fibre [21], which explains the two phenomena mentioned above.

Table 2. Hysteresis area for the three different samples: Native, Gamma and US 30 min.

Samples	Hysteresis Area
Native	149
Gamma	73
US 30 min	96

3.4. SEM Observations for a Flax-PLA Preform

Figure 8 shows the structure of non-woven preforms. Flax tows are mainly composed of flax fibre bundles but also of low amounts of residual shives originating from the woody part of the stem (Figure 8a). The flax tows used have a contaminant level (shives) less than 5%. Figure 8b illustrates the flax and PLA fibres that constitute the flax-PLA preforms used in the manufacture of non-woven flax-PLA composites. During composite manufacturing, flax and PLA fibres tend to align in the machine direction (Figure 8c). This is why the mechanical behaviour of non-woven composites was tested using both the machine and cross directions.

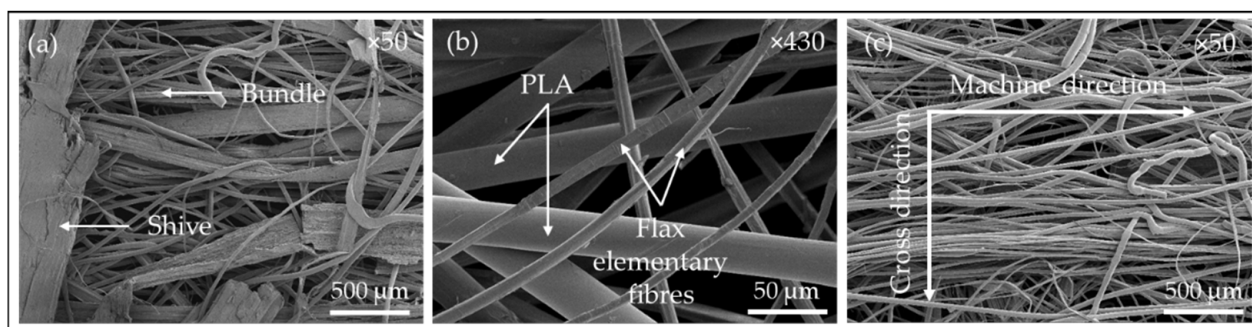


Figure 8. SEM observations for (a) Flax tows; (b,c) Flax-PLA preform.

3.5. Porosity Content for Flax-PLA Interface of Non-Woven Composites

The cross-sections of the non-woven composites were investigated using SEM, as shown in Figure 9. By eye, contrasting porosities are observed among the different non-woven composites. Figure 9a,b illustrate the presence of porosities inside the Native and Gamma composites, respectively. In contrast, the US 30 min sample does not present porosity (Figure 9c).

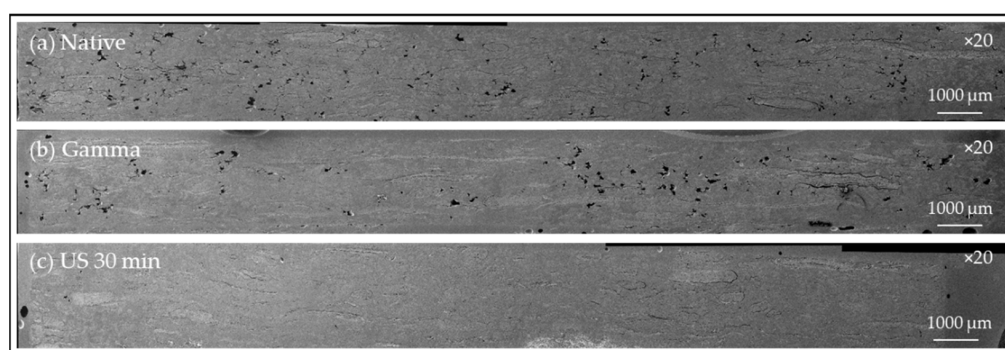


Figure 9. SEM observations of non-woven composites (a) Native; (b) Gamma; (c) US 30 min.

To quantify the porosity content, an image analysis of the cross-section was performed, and the results obtained are summarised in Table 3.

Table 3. Porosity content of the non-woven composites according to the card machine orientation.

Samples	Main Flax Direction	Porosity Content (%)
Native	Machine direction	2.8 ± 0.9
	Cross direction	5.1 ± 1.8
Gamma	Machine direction	2.9 ± 1.7
	Cross direction	4.7 ± 2.5
US 30 min	Machine direction	0.4 ± 0.1
	Cross direction	0.5 ± 0.3

Image analysis confirms that the US 30 min composite has very little porosity with values of 0.4% and 0.5% in the machine and cross directions, respectively. On the other hand, the two other non-woven composites, Native and Gamma, show porosities of 2.8% and 2.9% in the machine direction, respectively. These porosities are even greater in the cross direction, with values reaching 5.1% and 4.7% for the Native and Gamma samples, respectively.

3.6. Mechanical Properties of Non-Woven Composites

The results from machine and cross direction tensile tests on non-woven composites are summarised in Figure 10. For the machine direction, Young's modulus for the Native sample is the highest at 15.9 GPa (Figure 10a) compared to 13.1 and 13.7 GPa for the Gamma and US 30 min samples, respectively. On the other hand, the US 30 min sample shows the highest strength at 116 MPa, corresponding to an increase in stress of more than 10% at break compared to the Native sample (Figure 10b). For the Gamma sample, the stress at break is lower than that of the Native sample, with a decrease of approximately 13% from 106.3 to 94.5 MPa. Potential degradation of fibres due to exposure to gamma irradiation may result in poor mechanical properties. Regarding the strain at break (Figure 10c), there were no differences observed between the three samples tested, with a relatively large standard deviation of approximately 1%. For the cross direction, the trends are almost the same as those observed in the machine direction. The US 30 min sample has a Young's modulus of 7.3 GPa, which is equivalent to that of the Native sample (Figure 10a). For the stress at break, an increase of 12% is observed for the US 30 min sample compared to the Native sample with values of 54.1 and 48.7 MPa, respectively (Figure 10b). The stress at break for the Gamma sample is still below that for the Native sample. Finally, the strain at break does not show any change, with an average value of approximately 1.1% (Figure 10c).

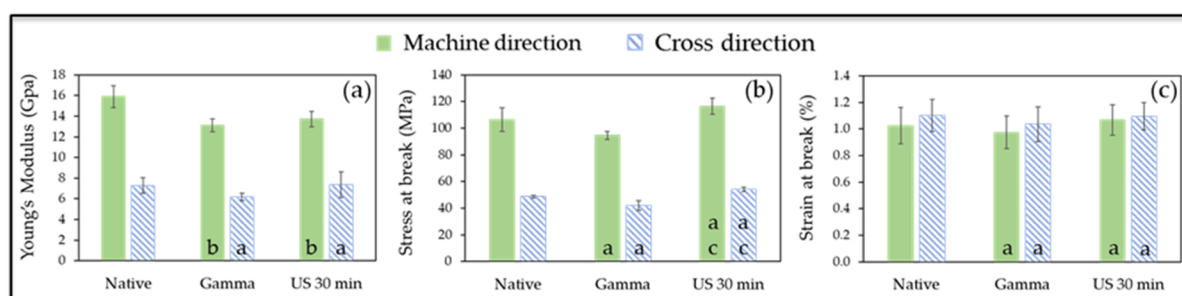


Figure 10. Tensile test results for (a) Young's modulus; (b) stress at break; (c) strain at break; Gamma column: If value is different compared to Native (p value < 0.05), letter b; otherwise letter a; US 30 min column: If value is different compared to Native, letter b otherwise letter a and if value is different compared to Gamma, letter c, otherwise left blank.

The results from the three-point bending tests for the non-woven composites are shown in Figure 11. The flexural modulus of the pre-treated tows, Gamma and US 30 min samples is lower than that for the Native composites with values of 7.1, 6.6 and 7.6 GPa, respectively (Figure 11a). Figure 11b indicates that the stress at break is very similar for the different composites, at approximately 140 MPa. On the other hand, the strain at break shows a value of 2.6% for the Gamma composite, which is the highest value obtained (Figure 11c). The strain at break is similar for the other two composites, Native and US 30 min, with values of 2.5% and 2.5%, respectively. The results in the cross direction are somewhat different. Indeed, the flexural modulus of the US 30 min composite is slightly higher than that of the Native composite at 5.2 and 5.0 GPa, respectively (Figure 11a). The Gamma composite shows a much lower flexural modulus of 3.0 GPa. The same trend is observed for the stress at break with values of 96.0, 90.1 and 53.8 MPa obtained for the US 30 min, Native and Gamma composites (Figure 11b). As for the tensile tests, the Gamma composites show the lowest mechanical properties, which can be attributed to degradation of the fibres by the pre-treatment. Finally, the strain at break shows relatively similar results in Figure 11c.

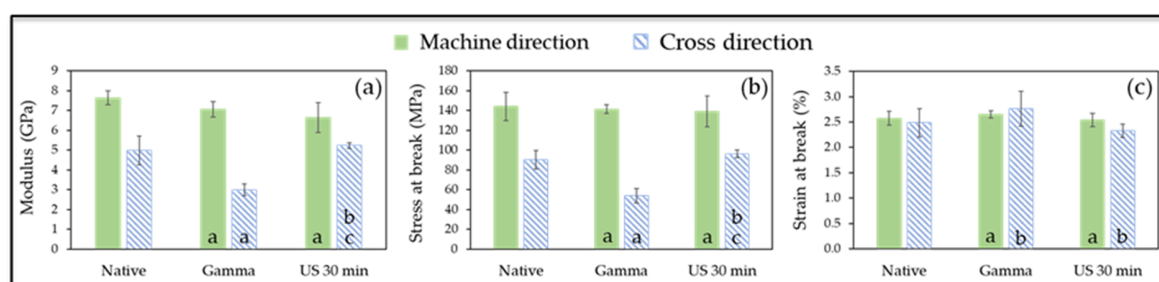


Figure 11. Bending tests results for (a) modulus; (b) stress at break; (c) strain at break ; Gamma column: If value is different compared to Native (p value < 0.05) letter b; otherwise letter a; US 30 min column: If value is different compared to Native, letter b otherwise letter a. In addition, if value is different compared to Gamma, letter c, otherwise left blank.

SEM observations of the fracture surface were performed for the different composites (Figure 12). Figure 12a shows the residual area of fibre bundle debonding generated by poor interfacial adhesion between the fibres and the matrix for the native non-woven composite. Another type of void is observable in Figure 12b again for the native composite. This is attributed to porosity because the surface of the matrix is much smoother than that found previously without any trace of fibre bundles. Figure 12c,d show the fibre–matrix interface for the US 30 min and Gamma composites, respectively. The US 30 min composite contains many elementary fibres that appear to be very well anchored within the matrix with narrow interstices between the two components. For the Gamma composite, a fibre bundle is perfectly visible in the centre of the image (Figure 12d). The fibre–matrix interface again looks good with no predominance of debonding. In general, voids produced by the debonding of a fibre bundle or an elementary fibre are mainly present for the Native composite, suggesting a possible positive effect of the treatments on polymer–fibre interfacial adhesion.

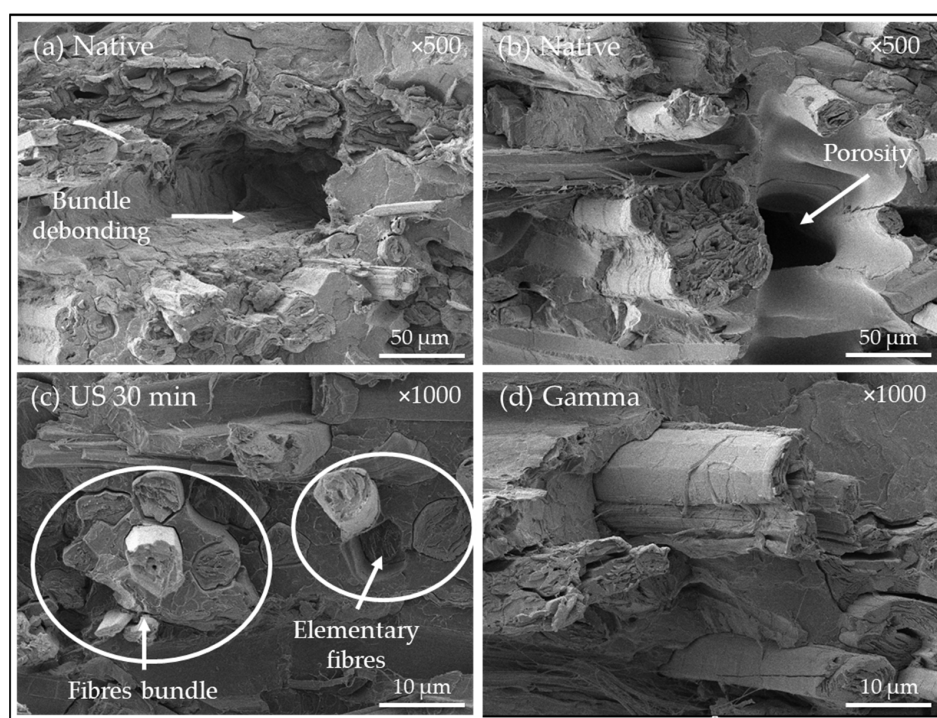


Figure 12. SEM observations of the interface of non-woven composites: (a) Debonding of fibre bundles; (b) porosity; (c,d) fibre bundles and elementary fibres in the US 30 min and Gamma composites, respectively.

3.7. Environmental Analysis of Pre-Treatments

Simplified environmental analysis was carried out to evaluate the environmental impacts of the two pre-treatments on flax tows. Figure 13 presents the results from the environmental analysis of flax tows pre-treated by ultrasound (US 30 min) and gamma irradiation (Gamma). Table 4 gathers the associated environmental impact values for native flax tows and energy consumption (fossil and nuclear) for the three studied tow batches.

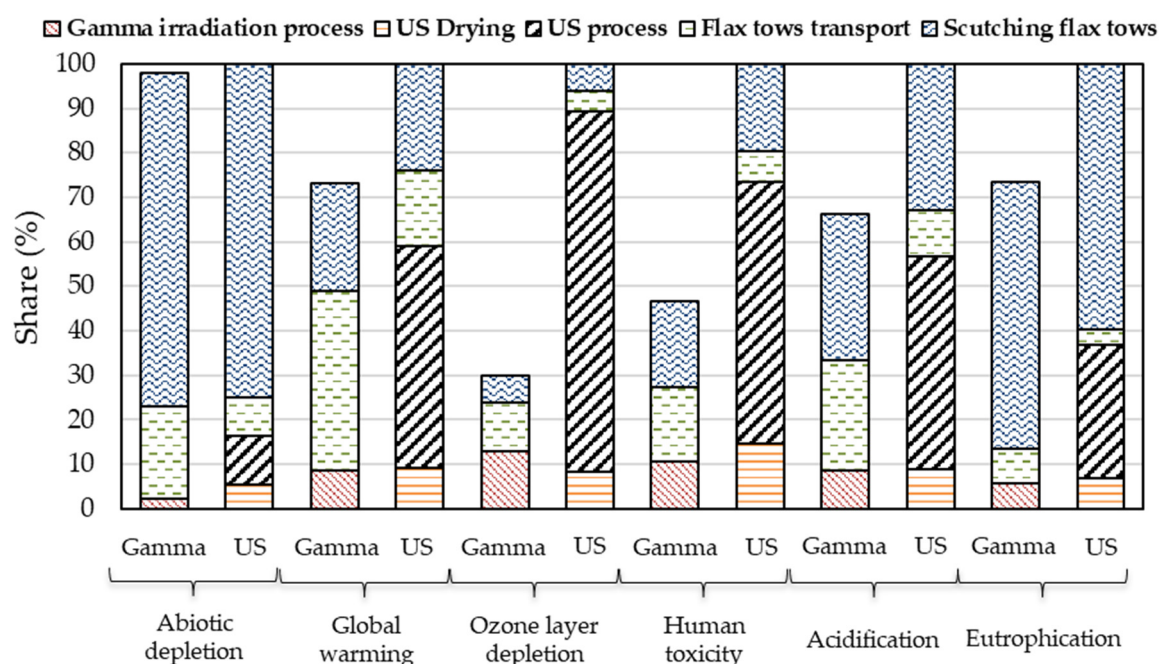


Figure 13. Normalised comparison of two fibre pre-treatments (Gamma and US 30 min) for six impact indicators decomposed according to the sources—scutching flax tows are included.

Table 4. Environmental impacts for the production of scutching native flax tows, flax tows pre-treated using the Gamma and US 30 min processes.

Impacts Category	Units	Untreated	Gamma	US 30 min
Abiotic depletion	kg Sb eq./kg	1.88×10^{-5}	2.46×10^{-5}	2.51×10^{-5}
Global warming (GWP100a)	kg CO ₂ eq./kg	1.24×10^{-1}	3.76×10^{-1}	5.14×10^{-1}
Ozone layer depletion (ODP)	kg CFC 11 eq./kg	2.13×10^{-8}	1.05×10^{-7}	3.50×10^{-7}
Human toxicity	kg 1.4 DB eq./kg	1.08×10^{-1}	2.57×10^{-1}	5.51×10^{-1}
Acidification	kg SO ₂ eq./kg	6.54×10^{-4}	1.32×10^{-3}	1.99×10^{-3}
Eutrophication	kg PO ₄ eq./kg	8.08×10^{-4}	9.92×10^{-4}	1.35×10^{-3}
Energy consumption, fossil	MJ/kg	1.43	5.31	6.95
Energy consumption, nuclear	MJ/kg	0.78	6.24	38.2

Analysis of the results highlights the environmental interest of gamma irradiation compared to ultrasound. From Figure 13, for gamma irradiation compared to US 30 min, we observe the following: Abiotic depletion is equivalent, global warming is reduced by 27%, ozone layer is depleted by 70%, human toxicity by 53%, acidification by 34% and eutrophication by 27%. This difference is mainly due to the US process: Driven by its higher power consumption (Table 4), the US process gives considerably higher values for all the indicators than Gamma process. Furthermore, for the case of US 30 min, the flax tows must be dried. Despite this, it should be noted that transport is more impactful for Gamma than US 30 min composites because of the distance travelled from the tow production site to the treatment site (2×639 km versus 2×267 km). These observations are visible

in the energy consumption of each treatment. Fossil energy consumption is similar for the two pre-treatments (5.31 MJ/kg for Gamma versus 6.95 MJ/kg for US 30 min). The US 30 min process consumes much more energy (mainly in the form of electricity usage) than the gamma process. Because the French electricity mix is composed of 70% nuclear power, nuclear energy consumption is significantly more important for US 30 min than gamma irradiation (38.22 against 6.24 MJ/kg). In addition, as shown in Table 4, for all the indicators, untreated flax tows are less impacted than flax tows treated by US 30 min or Gamma. In addition, US 30 min- and gamma-treated flax tows use four times more fossil energy and nine to 45 times more nuclear energy than untreated flax tows. The energy consumption for the untreated flax tows is of the same order of magnitude as reported in the literature [33].

To consider the mechanical aspect of the untreated and pre-treated flax tows, the previous results were weighted by the experimental maximum stress at break values for the PLA composite reinforced by the respective flax tows. To that end, a weight value (given in Table 5) was assigned to each case. The results are shown in Figure 14.

Table 5. Maximum stress values of PLA composite reinforced by respective flax-tows and corresponding weight values of scutching native and pre-treated flax tows by Gamma and US 30 min.

Flax-Tow Pre-Treatment	Maximum Stress (MPa)	Standard Deviation (MPa)	Weight Value
Native	106.3	8.8	1.09
Gamma	94.6	3.1	1.23
US 30 min	116.4	6.0	1.00

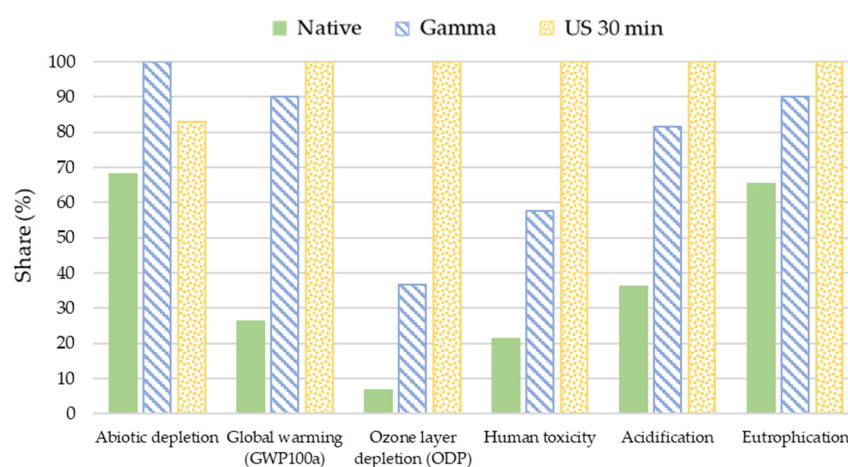


Figure 14. Normalised comparison of scutching native flax tows, flax tows pre-treated by Gamma and US 30 min for six impact indicators—weighted by the experimental maximum stress values obtained for the PLA composite reinforced by respective flax-tows.

The weight value was lower for the US 30 min composite compared with the untreated gamma composite. These differences result in a smaller gap between the US 30 min and Gamma processing than that shown in Figure 13. Despite this, Gamma irradiation remains less impactful than ultrasound pre-treatment, except for abiotic depletion. Moreover, even with a weight value based on maximal stress, the untreated flax tows show less environmental impact than that for the two studied pre-treatments.

4. Discussion

The impact of the two pre-treatments, Gamma irradiation and ultrasound applied to flax tows, was investigated at the tow scale and then at the composite material scale.

The increased individualisation of raw fibres, and; therefore, the increased number of elementary fibres after the two pre-treatments corroborates the biochemical results

with an elimination of the hemicellulosic and pectic compounds belonging to the middle lamella and/or the primary wall [34]. Indeed, it has been shown that gamma irradiation strongly degrades the middle lamella as well as the outer layer of fibres corresponding to the primary wall, even for low gamma irradiation doses, <10 kGy [28]. Even if only partial, the elimination of compounds ensuring the cohesion of fibre bundles explains the decrease in the number of fibre bundles observed in the morphological analysis. Thus, the differences in sorption-desorption capacity in DVS illustrated in Figure 7 can be explained by the removal of hydrophilic components, leading to individualisation of the pre-treated tows. Moisture absorption is greater for a fibre bundle than for an elementary fibre. Indeed, the pectins present in the middle lamella consist of carboxyl groups known to be highly polar and capable of forming hydrogen bonds with polar solvents such as water [35]. In our study, this can be explained by the native fibres, which have more fibre bundles. At the fibre scale, hemicelluloses contribute to the hydrophilic nature of fibres. Loss of hemicelluloses following pre-treatment affects the hygroscopic behaviour of fibres by reducing their ability to interact with water molecules. Indeed, hemicellulosic compounds are composed of hydrophilic hydroxyl groups. Amorphous hemicelluloses are largely responsible for the hydrophilic nature of flax fibres and their capacity to sorb water within the cell walls [36]. The presence of hysteresis on the sorption-desorption curves indicates the presence of mesopores in the structure of the fibre [37]. Indeed, flax fibres have a porous structure with many exchange surfaces. In addition, during desorption, water can be trapped inside the mesopores of the fibres. The decrease in the area of the hysteresis for the two pre-treatments could then suggest a phenomenon based on pore closure generated by collapse resulting from the pre-treatments. Coupled with the removal of hydrophilic compounds, the decrease in the hysteresis area also indicates a decrease in the number of water sorption and retention sites [32]. Hysteresis is particularly associated with relaxation during sorption. Its reduction; therefore, indicates a significant change in structure, probably linked to the elimination of certain hygroscopic compounds.

Regarding the mechanical properties of a non-woven flax-PLA composite, the maximum strength was measured to be 90.4 ± 7.8 MPa [38]. Apart from the 10% increase in the tensile strength for the US 30 min composite, no significant gain for the Young's modulus and the elongation at break was observed for the US 30 and Gamma composites. In other words, the increase in the number of elementary fibres and in the specific interfacial area between the matrix and the flax fibres had no significant positive impact or was not sufficient to improve the final mechanical properties of the non-woven composites. These results may appear to be surprising at first. Indeed, fibre individualisation is considered an important parameter in the final mechanical properties of a composite material. It has been shown that greater individualisation generates better strength at break for a UD flax-epoxy composite for fibre volume fractions of 22%, 42% and 51% [19]. The two pre-treatments increase the number of fibre-matrix interfaces within the composite material, and, potentially, the quality of the fibre-matrix interface and load transfer between the matrix and the reinforcements during mechanical stress. Questions about the impact of the pre-treatments on the fibre-matrix interfacial shear strength are not addressed here. This interface can be characterised through different techniques and at different scales: Micro or macro scale corresponding here to the fibre scale or composite scale, respectively. The fibre-matrix interface could be tested at the microscale via microdroplet tests to obtain the interfacial shear strength (IFSS) [39]. In addition, tests have been performed at the interface between flax fibres and PLA with an IFSS value that has been measured for flax fibres and PLA [40]. IFSS was determined to be equal to 15.6 ± 2.7 MPa. It would then be interesting to compare this value with that for Native and pre-treated flax tows, and the poor mechanical properties of the Gamma composite may be potentially due to a poor-quality fibre-matrix interface. However, this may also be due to the degradation of fibres during pre-treatment which induces poor mechanical properties. Indeed, the changes occurring at the surface of the irradiated tows can induce changes in the adhesion between the fibre and polymer matrix. In addition, contact angle tests can allow better characterisation of the surface of

flax fibres via determination of the surface energies. It is possible to perform these tests with several solvents, such as water (to assess the hydrophilic or hydrophobic character), diiodomethane or even hexane [41].

However, it is also important to note that the mechanical properties are always better after US pre-treatment in the cross direction for both tensile and flexural tests. Because flax fibres are preferably oriented in the machine direction, they are oriented perpendicular to the axis of mechanical stress. In other words, in the cross direction, the fibre–fibre interfaces are more loaded; that is, the polymers belong to the middle lamella and the primary wall. Better mechanical properties in the cross direction result in stronger fibre–fibre interfaces equivalent to more elementary fibres, and; therefore, better individualisation. Thus, in our case, the positive impact of US is more pronounced in the transverse direction due to the strong impact of the quality of the interface on the transverse properties. When longitudinal properties are considered, fibre properties are more impactful due to the high orientation level of our materials [42]. This difference between transverse and longitudinal behaviour is clearly confirmed by the composite mechanical performances.

Obviously, the mechanical properties are much better in the longitudinal direction of the fibres than in the transverse direction, confirming literature data and the impact of fibre properties according to the considered direction. For example, for a UD flax-PLA composite, Young's modulus in the longitudinal and transverse directions is estimated to be 20.1 ± 2.8 and 4.2 ± 0.4 GPa, respectively [40]. Here, the best value for Young's modulus in the longitudinal direction for Native composites is 15.9 ± 1.0 GPa, which, interestingly, is not far from the UD value. On the other hand, in the cross direction, Young's modulus for the Native and US 30 min composites is equal to 7.3 ± 0.8 and 7.4 ± 1.3 GPa, respectively; these low values confirm the minor contribution of flax fibres in this direction and the high impact of the interface.

Generally, interfacial properties and fibre orientation highly influence the composite mechanical properties, but the porosity content and intrinsic properties of fibres must also be considered to better understand the moderate impact of fibre individualisation on the final composite performance. It would then be interesting to assess the fibre properties after the treatment stage. Indeed, a possible counterbalance effect is possible between the increase in individualisation and a potential degradation of fibre properties. Tensile tests for single fibres would make it possible to observe whether or not pre-treatments results in degradation of mechanical properties. It may also be interesting to focus on the microstructure of the fibres to observe any reorganisation of the wall polymers and the creation of cavities. The most suitable technique for this type of scale analysis is nuclear magnetic resonance, possibly coupled with mechanical Atomic Force Microscope Peakforce investigations, to assess the impact of treatments on cell wall properties and ultrastructure. Finally, one must keep in mind the impact of porosity on composite mechanical properties; a very low porosity content is achieved for US-treated composites, which also has an impact on performance and can partially explain the improved mechanical properties for this composite. This can raise debate and questions about the exact impact of treatments. For the two other materials, the porosity content is high and suggests possible packing issues and limits in fibre content, especially when low-pressure processing tools, such as thermocompression, are used.

The environmental analysis applied to the two pre-treatments shows a significant impact of these pre-treatments through different environmental indicators. In addition, the gain provided by the pre-treatments for the mechanical properties of non-woven composites remains low compared to the impact on the environment. In other words, our pre-treatments do not currently appear to be a credible and environmentally friendly alternative to increase the mechanical properties of composite materials. However, gamma pre-treatment shows lower environmental indicators. Thus, pre-treatments that do not involve immersion, and; therefore, do not involve a drying step, are favoured. Nevertheless, the range of pre-treatments available without immersion and without the use of chemicals is not that wide, strongly restricting choice. In addition, this type of pre-treatment can

instead be used to improve the fibre–matrix interface by considerably modifying the surface of natural fibres. For example, there exists plasma pre-treatment, UV pre-treatment or steam explosion, among others [22,43].

5. Conclusions

The impact of ultrasound and gamma irradiation pre-treatment was investigated at the scale of tows and non-woven composite materials. Morphological analysis showed better individualisation for pre-treated tows, with a 20% increase in elementary fibres for gamma irradiation and a more than 15% increase for ultrasound pre-treatment. Both pre-treatments partially removed the middle lamella responsible for the cohesion of the fibre bundles, as targeted. Consequently, hemicellulosic and pectic components known to belong to the middle lamella were also removed, which also impacted the sorption-desorption behaviour of flax tow. Both pre-treatments showed a decrease in water uptake behaviour. At the non-woven composite scale for the tensile test, a 10% increase in stress at break for the US 30 min composite in the machine direction was observed. However, no improvement in Young's modulus or elongation at break was observed for Gamma and US 30 min composites compared to the Native composite. Fine quantification of the porosity in the non-woven composites showed that the ultrasound pre-treatment displays a lower porosity content, arguably leading to the observation of a slight mechanical improvement for non-woven flax-PLA composites. Finally, environmental analysis showed that if any additional pre-treatment weighs down the environmental balance compared to native tows, gamma irradiation is much more suitable than US processing.

Author Contributions: Conceptualization, M.G., F.G., A.B. and J.B.; Investigation, M.G., G.B. and T.C.; Supervision, F.G., A.B. and J.B.; Validation, F.G., A.B. and J.B.; Writing—original draft, M.G.; Writing—review & editing, M.G., A.K., G.B., F.D., T.C., F.P., M.H., N.L.M., F.G., A.B. and J.B. All authors have read and agreed to the published version of the manuscript.

Funding: This research was funded by by Interreg V.A Cross-Channel Programme through, FLOWER: Flax composites, LOW weight, End of life and Recycling (<http://flower-project.eu>), Grant No. 23) and Pays de la Loire region.

Institutional Review Board Statement: Not Applicable.

Informed Consent Statement: Not applicable.

Data Availability Statement: Not Applicable.

Acknowledgments: We thank Sylviane Daniel (INRAe Nantes) for the monosaccharide results and analysis. We also thank Antohny Magueresse (Univ Bretagne Sud) for the different SEM observations and Bastien Watbled (Littoral Côte d'Opale University) for its availability during ultrasound pre-treatment.

Conflicts of Interest: The authors declare no conflict of interest.

References

1. Le Gall, M.; Davies, P.; Martin, N.; Baley, C. Recommended flax fibres density values for composite property predictions. *Ind. Crop. Prod.* **2018**, *114*, 52–58. [CrossRef]
2. Lefeuvre, A.; Bourmaud, A.; Morvan, C.; Baley, C. Tensile properties of elementary fibres of flax and glass: Analysis of reproducibility and scattering. *Mater. Lett.* **2014**, *130*, 289–291. [CrossRef]
3. Beaugrand, J.; Berzin, F. Lignocellulosic fiber reinforced composites: Influence of compounding conditions on defibrization and mechanical properties. *J. Appl. Polym. Sci.* **2013**, *128*, 1227–1238. [CrossRef]
4. Joshi, S.V.; Drzal, L.T.; Mohanty, A.K.; Arora, S. Are natural fiber composites environmentally superior to glass fiber reinforced composites? *Compos. Part A Appl. Sci. Manuf.* **2004**, *35*, 371–376. [CrossRef]
5. Nuez, L.; Gautreau, M.; Mayer-Laigle, C.; d'Arras, P.; Guillon, F.; Bourmaud, A.; Baley, C.; Beaugrand, J. Determinant morphological features of flax plant products and their contribution in injection moulded composite reinforcement. *Compos. Part C* **2020**, *3*, 100054.
6. Van de Velde, K.; Kiekens, P. Thermoplastic polymers: Overview of several properties and their consequences in flax fibre reinforced composites. *Polym. Test.* **2001**, *20*, 885–893. [CrossRef]
7. Bledzki, A.K.; Faruk, O.; Sperber, V.E. Cars from bio-fibres. *Macromol. Mater. Eng.* **2006**, *291*, 449–457. [CrossRef]

8. Bourmaud, A.; Shah, D.U.; Beaugrand, J.; Dhakal, H.N. Property changes in plant fibres during the processing of bio-based composites. *Ind. Crop. Prod.* **2020**, *154*, 112705. [\[CrossRef\]](#)
9. Ramakrishnan, K.; Le Moigne, N.; De Almeida, O.; Regazzi, A.; Corn, S. Optimized manufacturing of thermoplastic biocomposites by fast induction-heated compression moulding: Influence of processing parameters on microstructure development and mechanical behaviour. *Compos. Part A Appl. Sci. Manuf.* **2019**, *124*, 105493. [\[CrossRef\]](#)
10. Kushwaha, G.S.; Sharma, N.K. Green initiatives: A step towards sustainable development and firm's performance in the automobile industry. *J. Clean. Prod.* **2016**, *121*, 116–129. [\[CrossRef\]](#)
11. Bourmaud, A.; Beaugrand, J.; Shah, D.U.; Placet, V.; Baley, C. Towards the design of high-performance plant fibre composites. *Prog. Mater. Sci.* **2018**, *97*, 347–408. [\[CrossRef\]](#)
12. Wang, C.; Wang, N.; Liu, S.; Zhang, H.; Zhi, Z. Investigation of microfibril angle of flax fibers using X-ray diffraction and SEM. *J. Nat. Fibers* **2018**. [\[CrossRef\]](#)
13. Zamil, M.S.; Geitmann, A. The middle lamella-more than a glue. *Phys. Biol.* **2017**, *14*, 11. [\[CrossRef\]](#) [\[PubMed\]](#)
14. Nuez, L.; Beaugrand, J.; Shah, D.U.; Mayer-Laigle, C.; Bourmaud, A.; D'arras, P.; Baley, C. The potential of flax shives as reinforcements for injection moulded polypropylene composites. *Ind. Crops Prod.* **2020**, *148*, 13. [\[CrossRef\]](#)
15. Buranov, A.U.; Mazza, G. Extraction and characterization of hemicelluloses from flax shives by different methods. *Carbohydr. Polym.* **2010**, *79*, 17–25. [\[CrossRef\]](#)
16. Shah, D. Natural fibre composites: Comprehensive ashby-type materials selection charts. *Mater. Des.* **2014**, *62*, 21–31. [\[CrossRef\]](#)
17. Melelli, A.; Arnould, O.; Beaugrand, J.; Bourmaud, A. The middle lamella of plant fibers used as composite reinforcement: Investigation by atomic force microscopy. *Molecular* **2020**, *25*, 632. [\[CrossRef\]](#)
18. Bourmaud, A.; Ausias, G.; Lebrun, G.; Tachon, M.-L.; Baley, C. Observation of the structure of a composite polypropylene/flax and damage mechanisms under stress. *Ind. Crop. Prod.* **2013**, *43*, 225–236. [\[CrossRef\]](#)
19. Coroller, G.; Lefeuvre, A.; Le Duigou, A.; Bourmaud, A.; Ausias, G.; Gaudry, T.; Baley, C. Effect of flax fibres individualisation on tensile failure of flax/epoxy unidirectional composite. *Compos. Part A Appl. Sci. Manuf.* **2013**, *51*, 62–70. [\[CrossRef\]](#)
20. Le Moigne, N.; Sonnier, R.; El Hage, R.; Rouif, S. Surfaces and Interfaces in Natural Fibre Reinforced Composites: Fundamentals, Modifications and Characterization. In *Surfaces and Interfaces in Natural Fibre Reinforced Composites: Fundamentals, Modifications and Characterization*; Springer: Berlin, Germany, 2018; p. 1.
21. Liu, M.; Meyer, A.S.; Fernando, D.; Silva, D.A.S.; Daniel, G.; Thygesen, A. Effect of pectin and hemicellulose removal from hemp fibres on the mechanical properties of unidirectional hemp/epoxy composites. *Compos. Part A Appl. Sci. Manuf.* **2016**, *90*, 724–735. [\[CrossRef\]](#)
22. Kalia, S.; Kaith, B.; Kaur, I. Pretreatments of natural fibers and their application as reinforcing material in polymer composites-A review. *Polym. Eng. Sci.* **2009**, *49*, 1253–1272. [\[CrossRef\]](#)
23. Fernandez, J.A.; Le Moigne, N.; Caro-Bretelle, A.S.; El Hage, R.; Le Duc, A.; Lozachmeur, M.; Bono, P.; Bergeret, A. Role of flax cell wall components on the microstructure and transverse mechanical behaviour of flax fabrics reinforced epoxy biocomposites. *Ind. Crops Prod.* **2016**, *85*, 93–108. [\[CrossRef\]](#)
24. Borsa, J.; László, K.; Boguslavsky, L.; Takacs, E.; Rácz, I.; Tóth, T.; Szabó, D. Effect of mild alkali/ultrasound treatment on flax and hemp fibres: The different responses of the two substrates. *Cellulose* **2016**, *23*, 2117–2128. [\[CrossRef\]](#)
25. Ghosh, R.; Ramakrishna, A.; Reena, G. Effect of air bubbling and ultrasonic processing on water absorption property of banana fibre-vinylester composites. *J. Compos. Mater.* **2013**, *48*, 1691–1697. [\[CrossRef\]](#)
26. Subhedar, P.B.; Gogate, P.R. Alkaline and ultrasound assisted alkaline pretreatment for intensification of delignification process from sustainable raw-material. *Ultrason. Sonochem.* **2014**, *21*, 216–225. [\[CrossRef\]](#)
27. Choi, H.Y.; Han, S.O.; Lee, J.-S. The Effects of Morphological Properties of Henequen Fiber Irradiated by EB on the Mechanical and Thermal Properties of Henequen Fiber/PP Composites. *Compos. Interfaces* **2009**, *16*, 751–768. [\[CrossRef\]](#)
28. Le Moigne, N.; Sonnier, R.; El Hage, R.; Rouif, S. Radiation-induced modifications in natural fibres and their biocomposites: Opportunities for controlled physico-chemical modification pathways? *Ind. Crop. Prod.* **2017**, *109*, 199–213. [\[CrossRef\]](#)
29. Khan, R.A.; Khan, M.A.; Khan, A.H.; Hossain, M.A. Effect of gamma radiation on the performance of jute fabrics-reinforced polypropylene composites. *Radiat. Phys. Chem.* **2009**, *78*, 986–993.
30. Quémener, B.; Bertrand, D.; Marty, I.; Causse, M.; Lahaye, M. Fast data preprocessing for chromatographic fingerprints of tomato cell wall polysaccharides using chemometric methods. *J. Chromatogr. A* **2007**, *1141*, 41–49. [\[CrossRef\]](#)
31. Hauschild, M.G.M.; Guinee, J.; Heijungs, R.; Huijbregts, M.; Joliet, O.; Margni, M.; De Schryver, A.; Pennington, D.; Pant, R.; Sala, S.; et al. *Recommendations for Life Cycle Impact Assessment in the European Context—Based on Existing Environmental Impact Assessment Models and Factors (International Reference Life Cycle Data System—ILCD Handbook)*; EUR 24571 EN; Luxembourg Publications Office of the European Union: Luxembourg, 2011.
32. Salmén, L.; Larsson, P.A. On the origin of sorption hysteresis in cellulosic materials. *Carbohydr. Polym.* **2018**, *182*, 15–20. [\[CrossRef\]](#)
33. Le Duigou, A.; Davies, P.; Baley, C. Environmental impact analysis of the production of flax fibres to be used as composite material reinforcement. *J. Biobased Mater. Bioenergy* **2011**, *5*, 153–165. [\[CrossRef\]](#)
34. Lefeuvre, A.; Baley, C.; Morvan, C. Analysis of Flax Fiber Cell-Wall Non-Cellulosic Polysaccharides Under Different Weather Conditions (Marylin Variety). *J. Nat. Fibers* **2018**, *15*, 539–544. [\[CrossRef\]](#)
35. Celino, A.; Fréour, S.; Jacquemin, F.; Casari, P. The hygroscopic behavior of plant fibers: A review. *Front. Chem.* **2014**, *2*, 12.

-
36. Hill, C.A.S.; Norton, A.; Newman, G. The water vapor sorption behavior of natural fibers. *J. Appl. Polym. Sci.* **2009**, *112*, 1524–1537. [[CrossRef](#)]
 37. Padovani, J.; Legland, D.; Pernes, M.; Gallos, A.; Thomachot-Schneider, C.; Shah, D.; Bourmaud, A.; Beaugrand, J. Beating of hemp bast fibres: An examination of a hydro-mechanical treatment on chemical, structural, and nanomechanical property evolutions. *Cellulose* **2019**, *26*, 5665–5683. [[CrossRef](#)]
 38. Pantaloni, D.; Shah, D.; Baley, C.; Bourmaud, A. Monitoring of mechanical performances of flax non-woven biocomposites during a home compost degradation. *Polym. Degrad. Stab.* **2020**, *177*, 109166. [[CrossRef](#)]
 39. Miller, B.; Muri, P.; Rebenfeld, L. A microbond method for determination of the shear strength of a fiber/resin interface. *Compos. Sci. Technol.* **1987**, *28*, 17–32. [[CrossRef](#)]
 40. Pantaloni, D.; Rudolph, A.L.; Shah, D.U.; Baley, C.; Bourmaud, A. Interfacial and mechanical characterisation of biodegradable polymer-flax fibre composites. *Compos. Sci. Technol.* **2020**, *201*, 108529. [[CrossRef](#)]
 41. Pucci, M.F.; Liotier, P.J.; Seveno, D.; Fuentes, C.; Van Vuure, A.; Drapier, S. Wetting and swelling property modifications of elementary flax fibres and their effects on the Liquid Composite Molding process. *Compos. Part A Appl. Sci. Manuf.* **2017**, *97*, 31–40. [[CrossRef](#)]
 42. Gager, V.; Legland, D.; Bourmaud, A.; Le Duigou, A.; Pierre, F.; Behlouli, K.; Baley, C. Oriented granulometry to quantify fibre orientation distributions in synthetic and plant fibre composite preforms. *Ind. Crop. Prod.* **2020**, *152*, 7. [[CrossRef](#)]
 43. Liu, M.; Thygesen, A.; Summerscales, J.; Meyer, A.S. Targeted pre-treatment of hemp bast fibres for optimal performance in biocomposite materials: A review. *Ind. Crop. Prod.* **2017**, *108*, 660–683. [[CrossRef](#)]